Eggshell Matrix Protein Mimics: Designer Peptides to Induce the Nucleation of Calcite Crystal Aggregates in Solution

Parayil Kumaran Ajikumar,[†] Rajamani Lakshminarayanan,[‡] Boon Tee Ong,[§] Suresh Valiyaveettil,*[,†,‡] and R. Manjunatha Kini[⊥]

Singapore-MIT Alliance, Department of Chemistry, Department of Biological Sciences, and Chemical Process and Engineering Center, National University of Singapore, 3 Science Drive 3, Singapore 117543, Singapore

Received March 31, 2003; Revised Manuscript Received June 26, 2003

Ansocalcin is a novel goose eggshell matrix protein with 132 amino acid residues, which induces the formation of polycrystalline calcite aggregates in in vitro crystallization experiments. The central region of ansocalcin is characterized by the presence of multiplets of charged amino acids. To investigate the specific role of charged amino acid multiplets in the crystal nucleation, three short peptides REWD-16, REWDP-17 (containing charged doublets), and RADA-16 (alternating charged residues) were synthesized and characterized. The aggregation of these peptides in solution was investigated using circular dichroism, intrinsic tryptophan fluorescence, and dynamic light scattering experiments. The peptides REWD-16 and REWDP-17 induced the polycrystalline calcite crystal aggregates, whereas RADA-16 did not induce significant changes in calcite crystal morphology or aggregate formation in in vitro crystallization experiments. The lattice and morphology of the calcite crystals were characterized using X-ray diffraction and scanning electron microscope. The results discussed in this paper reveal the importance of multiplets of charged amino acid residues toward the nucleation of polycrystalline calcite crystal aggregates in solution.

Introduction

Avian eggshell is a biocomposite containing ca. 3.5% organic components (such as proteins and proteoglycans) and 95% inorganic phase (calcite phase).[1] It has been hypothesized that the intracrystalline biomacromolecules control the calcite crystal nucleation, growth morphology, and strengths of the shells.[2] A number of chicken eggshell matrix proteins have been isolated and characterized and are believed to play an important role in the eggshell calcification.[3] On the basis of the electron microscopy studies, Mann suggested that the nucleation of calcite crystals takes place in a regiospecific site located on the shell membrane.[4] These crystals subsequently grow until they become spatially restricted by the growing ends of adjacent crystals and by the proteins secreted into the palisade layer. Another hypothesis is that the structural organization is assisted by the organic matrix components or by the competitive crystal growth processes due to the presence of multiple nucleating sites.[5]

There have been many elegant approaches to devise biomineralization models for the $CaCO_3$ crystallization. Most of the earlier works using synthetic templates have addressed the role of acidic macromolecules or short peptides with acidic and neutral repeating residues on the $CaCO_3$ crystallization. Wheeler and Sikes[6] reported that peptides with a repeating Asp-Ala sequence and $(Asp)_n$ inhibited the crystallization of the $CaCO_3$ from solution. Wierzbicki et al.[7] observed that the binding of $(Asp)_{15}$ to the {11.0} faces of the calcite crystals mimics the properties of the oyster shell matrix protein. Levi et al.[8] tested a series of aspartic acid and leucine or glutamic acid and leucine containing synthetic peptides [poly(Asp-Leu), poly(Leu-Asp-Asp-Leu), poly(Glu-Leu), poly(Leu-Glu-Glu-Leu), poly(Asp), and poly(Glu)] as models to study the selective nucleation of calcite/aragonite polymorphism in mollusk shells. Their observation revealed that the polymorph specificity depends on the amino acid sequence, the conformation of specific peptides or proteins and the microenvironment of crystal nucleation and growth. DeOliveira et al.[9] designed an α-helical peptide with an array of aspartidyl residues to interact with specific crystal faces and suggested that the helical form of the peptide recognizes specific crystal faces, whereas the unfolded form acts nonspecifically as a polyanion. Recently, the feasibility of the phage display library of oligopeptides to identify the peptides with amino acid sequences capable of forming functional interactions with the $CaCO_3$ has been reported.[10]

Design of Peptides. In the biomineralization process, there have been a number of reports about the significant role of proteins to modify the microstructure of the inorganic mineral phases.[11] Recently, we reported the amino acid sequence of ansocalcin, the major protein present in the goose eggshell extract.[12] Ansocalcin showed high homology (38% identity and 52% similarity) to a chicken eggshell matrix protein, ovocleidin-17 (OC-17).[12b,13] Using in vitro crystal growth experiments, we have shown that ansocalcin induced the growth of polycrystalline aggregates of calcite crystals.[12] The concentration-dependent oligomerization of ansocalcin was

* To whom correspondence should be addressed. E-mail: chmsv@nus.edu.sg.
[†] Singapore-MIT Alliance.
[‡] Department of Chemistry.
[⊥] Department of Biological Sciences.
[§] Chemical and Process Engineering Center.

10.1021/bm034101b CCC: $25.00
Published on Web 08/14/2003

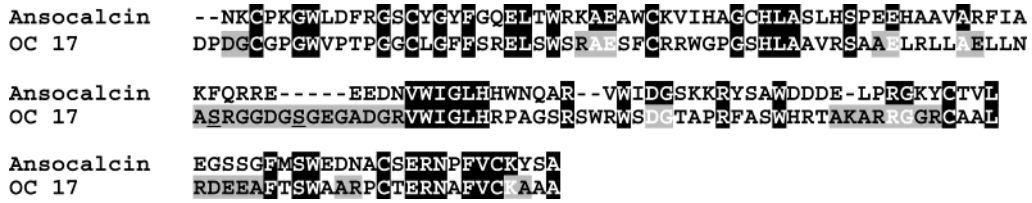

Figure 1. Alignment of the amino acid sequence of ansocalcin with OC-17. The identical amino acids are shaded in black. The two phosphoserines in OC-17 are underlined. The XY stretches in OC-17, where X = acidic or basic amino acids and Y = G or A (neutral amino acid residues), are shaded in gray. The important difference between the two sequences is the presence of acidic and basic multiplets in ansocalcin.

Table 1. Amino Acid Sequence and Observed and Theoretical Masses of the Synthetic Peptides

sequence	observed mass[a]	theoretical mass[b]
RREEWWDDRREEWWDD (REWD-16)	2364.20 ± 0.01	2364.43
RREEWWDDPRREEWWDD (REWDP-17)	2462.16 ± 0.02	2461.55
RADARADARADARADA (RADA-16)	1671.20 ± 0.02	1671.75

[a] Masses were determined by electrospray ionization mass spectrometry. [b] Masses were calculated using the Peptide Mass from http://tw.expasy.org/tools/peptide-mass.html.

suggested as a possible mechanism for the growth of calcite crystal aggregates. On the other hand, OC-17 did not alter the shape of $CaCO_3$ crystals (unpublished results). Thus, despite sharing a high homology, the interaction of the proteins with $CaCO_3$ crystals is different. In alignment of the amino acid sequences of ansocalcin and OC-17, considerable differences are observed in the central region (Figure 1). This region consists of many charged amino acid multiplets in ansocalcin, whereas an alternating pattern of charged and neutral amino acid residues is observed in OC-17 (colored gray in the Figure 1). Acidic and basic amino acid multiplets are present in a number of soluble matrix proteins associated with calcium-rich biominerals.[14] Molecular modeling studies indicated that such repetitive arrangements might be responsible for the nucleation and growth regulation of crystals.[14b] However, there has been no experimental evidence to elucidate the role of acidic and basic amino acid multiplets present in the soluble proteins that are involved in the mineralization of $CaCO_3$. In ansocalcin, there are two quartets (Glu^{63}-Glu^{64}-Glu^{65}-Asp^{66} and Asp^{93}-Asp^{94}-Asp^{95}-Glu^{96}) and two doublets (Glu^{47}-Glu^{48} and Glu^{116}-Asp^{117}) of acidic residues and one triplet (Lys^{86}-Lys^{87}-Arg^{88}) and three doublets (Arg^{25}-Lys^{26}, Arg^{61}-Arg^{62}, and His^{73}-His^{74}) of basic residues (Figure 1). It also contains eight tryptophan residues of which three residues precede the charged pairs.

On the basis of the differences observed in the amino acid sequences of ansocalcin and OC-17, we designed a model peptide with repeating charged amino acids (REWD-16, Table 1). It is well-known that a number of biomineral regulatory proteins and polypeptides contain proline-rich domains. Presence of proline limits the conformational flexibility, and the organisms utilize such proline-rich domains to form three-dimensional supramolecular structure in the extracellular matrix.[11,15,16] Thus, we incorporated a proline residue in the peptide REWDP-17 (Table 1). For a better understanding, we have chosen a known sapeptide RADA-16 with alternating charged and neutral residues.[17] We discuss the influence of these peptides on $CaCO_3$ crystallization and characteristics of their self-assembly in solution.

Experimental Section

Synthesis and Characterization of the Peptides. Fmoc-PAL-PEG-PS and all the N^{α}-Fmoc-L-amino acid pentafluorophenyl esters were purchased from Novabiochem, San Diego, CA. The peptides were synthesized using the Pioneer peptide synthesizer (Applied Biosystems) employing the N^{α}-Fmoc-L-amino acid pentafluorophenyl ester/HOBt coupling method. The peptides REWD-16, REWDP-17, and RADA-16 were assembled on an Fmoc-PAL-PEG-PS (0.18 mmol/g) resin. All of the peptides were synthesized at a 0.1 mmol scale using an extended cycle protocol. The peptides were deprotected and cleaved using a cleavage cocktail consisting of 90% trifluoroacetic acid (TFA), 2.5% phenol, 2.5% water, 2.5% thioanizole, and 2.5% ethanedithiol for 3 h at room temperature. The mixture was filtered and concentrated under reduced pressure. The peptide was precipitated using cold ether and centrifuged on an ultracentrifuge with repeated washing by cold ether to remove all reagents and other impurities. Finally, the peptides were lyophilized with 10% acetic acid solution and obtained as white powder. All peptides were purified using the Phenomenex (250 mm × 10 mm, 10 μm) C18 reverse-phase column using a BioCAD workstation. The solvent systems used for the purification are as follows: solvent A, 0.1% TFA, and solvent B, 0.1% TFA in 80% acetonitrile. A linear gradient (flow rate 2 mL/min) of 25%−50% B over 50 min was used. The peptide elution was monitored at 215 nm. The purity of the peptides was confirmed using analytical HPLC and ESI-MS measurements.

Crystal Growth Experiments. $CaCO_3$ crystals were grown on glass cover slips placed inside the $CaCl_2$ solution kept in a Nunc dish with 6 × 4 wells at 25 ± 1 °C. Typically, 1 mL of 7.5 mM $CaCl_2$ solution was introduced into the wells containing the cover slips and the whole set up was covered with aluminum foil with a few pinholes at the top. To study the role of synthetic peptides in the $CaCO_3$ crystallization, aliquots of peptides were dissolved in 7.5 mM $CaCl_2$ solution to prepare a series of solutions at the concentration range of 50 μg/mL to 2 mg/mL and introduced into each well with a glass cover slip. Crystals were grown inside a closed desiccator for 2 days by slow diffusion of gases released by the decomposition of ammonium carbonate crystals placed at the bottom of the desiccator. After 2 days, the slides were carefully lifted from the crystallization wells,

rinsed gently with Millipore water, air-dried at room temperature, and used for further characterization.

Dynamic Light Scattering (DLS). One hundred twenty microliters of the peptide solution (concentration of 5 mg/mL) was used to perform dynamic light scattering experiments using PDDLS/Batch (Precision Detectors, Franklin, MA) instrument. Intensity data from each sample were collected in five replicates and analyzed using the Precision Deconvolve program and yielded size-versus-fraction distribution plots.

Circular Dichroism Experiments. Circular dichroism experiments were performed using Jasco J 715 spectropolarimeter. The CD spectra of the peptides (concentration range of 50 μg/mL to 2 mg/mL) dissolved in 7.5 mM $CaCl_2$ solution or in water were collected in the wavelength range of 260−190 nm using a 0.1 mm sample cell. The instrument optics was flushed with 30 L/min of nitrogen gas. A total of three scans were recorded and averaged for each spectrum, and baseline was subtracted.

Fluorescence Spectroscopy. The fluorescence emission spectra were recorded on a Shimadzu RF-5301PC spectrofluorometer with the emission and excitation band-passes set at 3 nm. Spectra were recorded from 300 to 400 nm at an excitation wavelength of 295 nm using a scan rate of 50 nm/min. The fluorescence spectra of the peptides were recorded in 7.5 mM $CaCl_2$ solution and in water.

Scanning Electron Microscopy (SEM). SEM studies on the $CaCO_3$ crystals grown on glass plates were carried out using JEOL 2200 scanning electron microscope at 15/20 kV after sputter coating with gold to increase the conductivity.

X-ray Diffraction Studies. Powder and single-crystal X-ray diffraction studies on the crystals were carried out using D5005 X-ray diffractometer with Cu Kα radiation at 40 kV and 40 mA multisampler system. The crystals overgrown on glass plates were mounted on the plastic holder, and the diffraction studies were carried out. For the powder X-ray measurements, the crystals were slightly crushed using a mortar, placed on a plastic holder, and wetted with a drop of ethanol to form a continuous film.

Results and Discussion

Interaction of the Peptides with $CaCO_3$ Crystals. $CaCO_3$ crystals were grown on microscopy slides by slow diffusion of CO_2 (generated by the decomposition of ammonium carbonate) to the peptides dissolved in 7.5 mM $CaCl_2$ solution for 2 days inside a sealed desiccator. Figure 2 shows scanning electron micrographs revealing the changes in the morphology of calcite crystals grown in the presence of REWD-16. In the control experiments with no added peptide, exclusive nucleation of rhombohedral calcite crystals was observed (Figure 2A). At low concentrations (100 and 250 μg/mL) of the peptide, the sharp rhombohedral edges of the calcite crystals became truncated (Figure 2B,C). As the concentration was increased to 2 mg/mL, smaller polycrystalline calcite crystal aggregates were formed (Figure 2D−F). Incorporation of proline in the peptide sequence (REWDP-17) seems to alter the nature of interaction of the

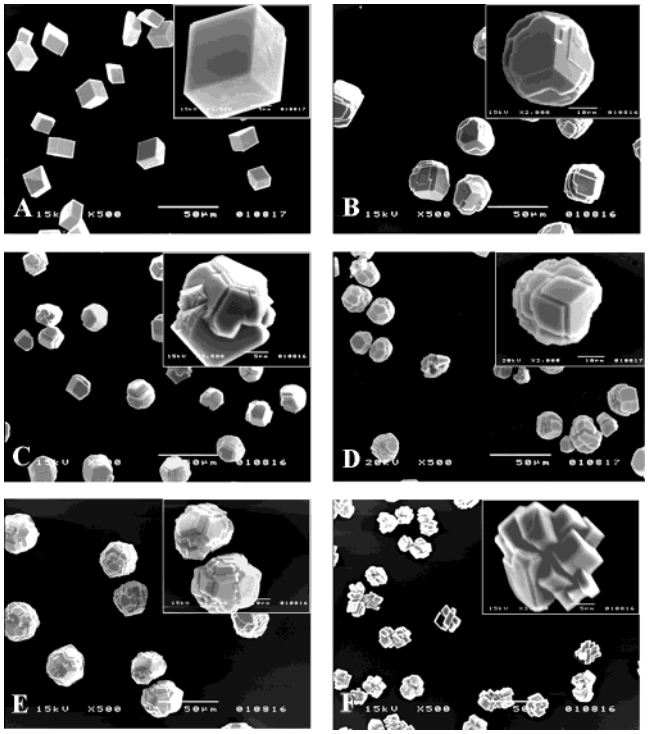

Figure 2. Representative electron micrograph of the calcite crystals grown in the presence of REWD-16. Concentrations of the peptide used were (A) 0.0 μg/mL, (B) 100 μg/mL, (C) 250 μg/mL, (D) 500 μg/mL, (E) 1 mg/mL, and (F) 2 mg/mL. Scale bar represents 50 μm.

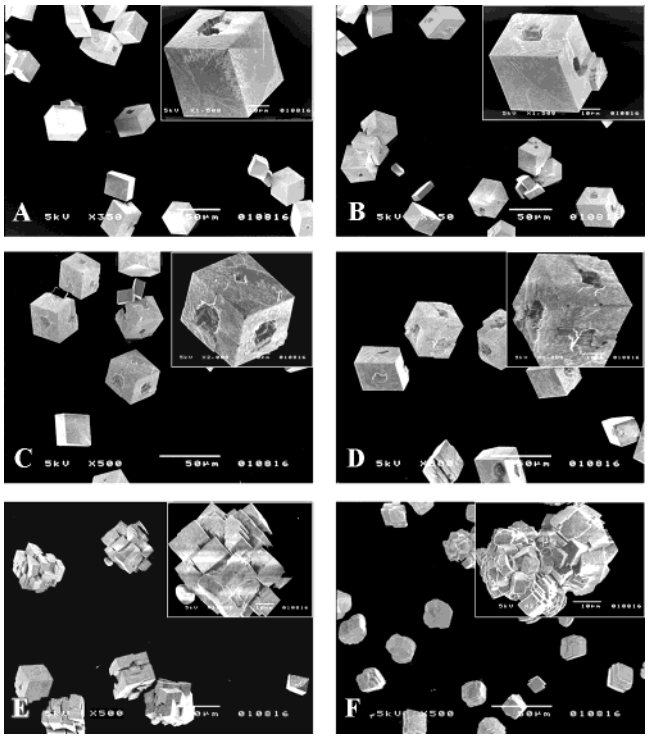

Figure 3. Representative electron micrograph of the calcite crystals grown in the presence of REWDP-17. Concentrations of the peptide used were (A) 50 μg/mL, (B) 100 μg/mL, (C) 250 μg/mL, (D) 500 μg/mL, (E) 1 mg/mL, and (F) 2 mg/mL. Scale bar represents 50 μm.

peptide with the growing crystals. Calcite crystals exhibiting screw dislocations were formed up to a concentration of 500 μg/mL (Figure 3A−D). At higher concentration of REWDP-17, the surface of the crystals was roughened, and at 1 mg/mL, polycrystalline aggregates were observed. These aggre-

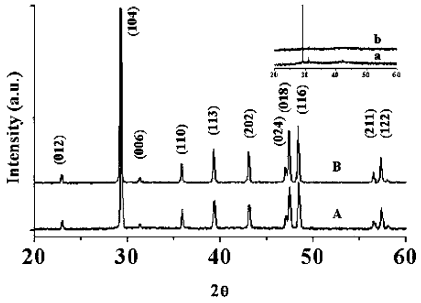

Figure 4. X-ray diffraction pattern of the powdered and single-crystal (inset) aggregates formed in the presence of 2 mg/mL of the peptides (A) REWD-16 and (B) REWDP-17.

gates consist of regularly ordered {10.4} rhombohedral crystallites (Figure 3E,F).

In the presence of both of the peptides, as the concentration increases, the mean crystal aggregate size was reduced from ~38 ± 5 μm (500 μg/mL) to 17 ± 3 μm (2 mg/mL) with an increase in nucleation density (number of crystals per unit area). Furthermore, in the calcite aggregates, the crystallite size was halved at higher concentration of the peptides (compare Figures 2E,F and 3E,F). X-ray diffraction of the crystal aggregates obtained showed a strong diffraction maxima at $2\theta \approx 30°$ that corresponds to {10.4}-faces of the rhombohedral crystallites (Figure 4, inset). In the powdered form, diffractions from all other crystal planes were observed indicating single-crystalline nature of the crystal aggregates (Figure 4A,B). Thus these peptides have shown the ability to induce the nucleation of multiple calcite crystals in a small area, thus promoting the formation of crystal aggregates with similar morphologies as those observed in the presence of ansocalcin. The sapeptide RADA-16, which mimics the central region of OC-17, had no influence either on the growth of calcite crystals or on the size or shape of the calcite crystals (Figure 5). These results strongly support the importance of charged residue multiplets in calcification of the goose eggshell.

Investigation of Solution Properties of the Peptides

Dynamic Light Scattering Studies. To obtain an insight into the structure of peptides in solution, we carried out dynamic light scattering studies at a concentration of 5 mg/mL for all three peptides. The hydrodynamic radius and the average diffusion coefficient calculated for these peptides are shown in the Table 2. Highly monodisperse particles with $\langle R_H \rangle$ ca. 3.3 nm were observed for REWD-16 (Figure 6A). This value was doubled (6.4 nm) upon proline incorporation, and the distribution was also broader for the peptide REWDP-17 (Figure 6B). The $\langle R_H \rangle$ for the RADA-16 was also found to be ca. 5.7 nm (Figure 6C). It is important to note that all three peptides (i.e., REWD-16, REWDP-17, and RADA-16) showed self-aggregation in solution. The average diffusion coefficient calculated for these peptides is comparable to the 15-kDa protein reported earlier.[18] Thus DLS studies indicated that all of the peptides exist as multimers in 7.5 mM $CaCl_2$.

Circular Dichroism (CD) Studies. The secondary structures of the peptides were studied using CD spectroscopy at

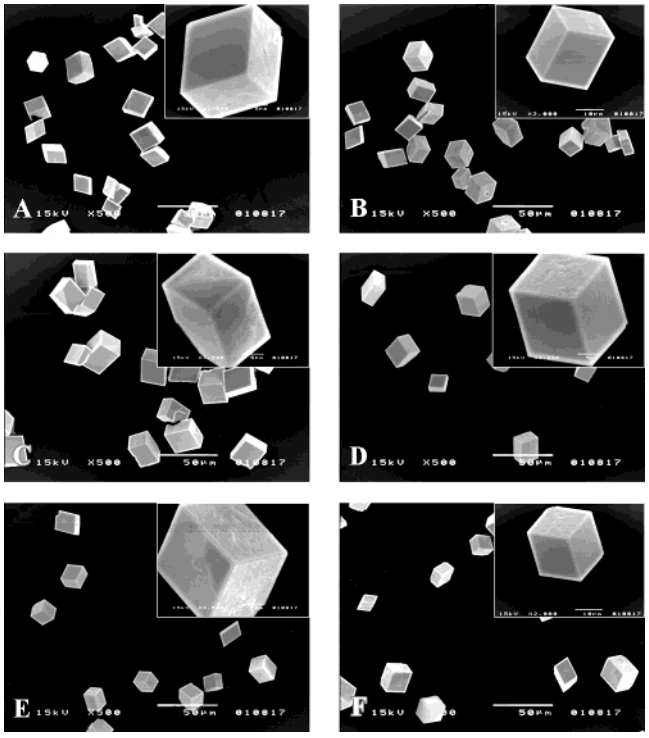

Figure 5. Representative electron micrograph of the calcite crystals grown in the presence of the peptide RADA-16. Concentrations of the peptide used were (A) 50 μg/mL, (B) 100 μg/mL, (C) 250 μg/mL, (D) 500 μg/mL, (E) 1 mg/mL, and (F) 2 mg/mL. Scale bar represents 50 μm.

Table 2. Average Diffusion Coefficient ($\langle D \rangle$) and Mean Hydrodynamic Radius ($\langle R_H \rangle$) of the Synthetic Peptides

peptides	$\langle D \rangle$ cm^2/s	$\langle R_H \rangle$ nm
REWD-16	8.80×10^{-7}	3.3
REWDP-17	4.62×10^{-7}	6.4
RADA-16	5.17×10^{-7}	5.7

25 °C in 7.5 mM $CaCl_2$ solution, as well as in water. All peptides exhibited strong changes in the secondary structure with change in peptide concentration in $CaCl_2$ solution (Figure 7). For REWD-16, the observed negative minimum at 217 nm and a positive maximum at 198 nm indicate a high degree of β-sheet conformation. As the concentration was increased, the amplitudes of the negative minimum and the positive maximum were increased. Incorporation of proline into the sequence (i.e., REWDP-17) resulted in the appearance of negative minimum at 227 nm, which indicates a β-turn conformation.[19] Increase in concentration of REWDP-17 resulted in a decrease of the negative minimum at 227 nm, followed by a red shift to 233 nm implying probable tryptophan−tryptophan interactions (Figure 7B). The CD spectra of RADA-16 in $CaCl_2$ solution showed a typical β-sheet conformation as reported by Zhang et al.[20] In water, no differences in the spectra were observed for the peptide REWD-16 up to 250 μg/mL. Above this level, excessive scattering complicated the analysis of the secondary structure. However, REWDP-17 exhibited high solubility in water and showed similar CD spectra as those observed in the presence of Ca^{2+} ions. These results confirm that the self-aggregation of peptides in solution is independent of Ca^{2+} ion concentrations in solution.

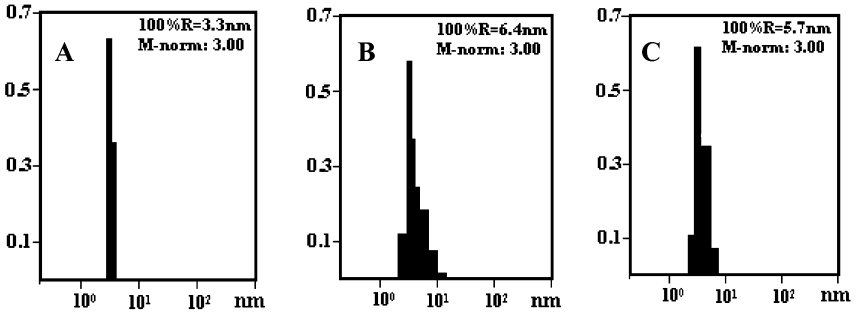

Figure 6. Particle size distribution of peptide aggregates in 7.5 mM $CaCl_2$ solution obtained by dynamic light scattering (DLS): (A) REWD-16; (B) REWDP-17; (C) RADA-16. *X*-axis indicates the size of the aggregates, and *Y*-axis represents the fraction distribution.

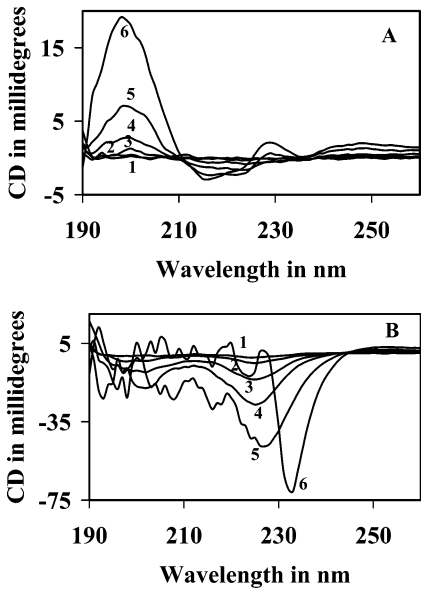

Figure 7. Circular dichroism spectra of the synthetic peptides (A) REWD-16 and (B) REWDP-17 in 7.5 mM $CaCl_2$ at various concentrations: (1) 50 μg/mL; (2) 100 μg/mL; (3) 250 μg/mL; (4) 500 μg/mL; (5) 1 mg/mL; (6) 2 mg/mL. CD spectra of peptide RADA-16 were published earlier by Zhang and Altman.[20] The instrument settings used were as follows: scan range, 190−260 nm; scan rate, 50 nm/min; sensitivity, 10 mdeg; response time, 1 s.

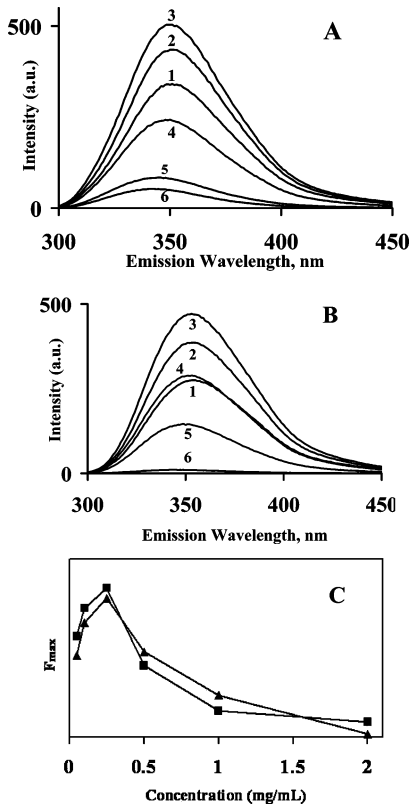

Figure 8. Intrinsic tryptophan emission spectra of the synthetic peptides (A) REWD-16 and (B) REWDP-17 at different concentrations. Note the decrease in intensity at higher concentrations (4−6) of the peptides. Concentrations of the peptides were (1) 50 μg/mL, (2) 100 μg/mL, (3) 250 μg/mL, (4) 500 μg/mL, (5) 1 mg/mL, and (6) 2 mg/mL. Panel C shows the emission intensity versus concentration profile of synthetic peptides REWD-16 at F_{max} = 350 nm (▲) and REWDP-17 at F_{max} = 357 nm (■) in 7.5 mM $CaCl_2$ solution. Emission intensity (*F*) is expressed in arbitrary units.

Fluorescence Studies. To understand the microenvironment around the tryptophan residues in the peptides REWD-16 and REWDP-17, we investigated the change in fluorescence emission characteristics of these peptides in 7.5 mM $CaCl_2$ solution and in water. Both peptides REWD-16 and REWDP-17 showed distinct emission characteristics (Figure 8A,B). The fluorescence emission maxima were observed at 353 and 357 nm for REWD-16 and REWDP-17, respectively, indicating the exposure of the fluorophores to polar environment. The intensity of emission maxima changes with change in peptide concentration (Figure 8). For REWD-16, the fluorescence intensity increased with increase in concentration up to 250 μg/mL and then decreased with a blue shift in the emission maximum to 345 nm at 2 mg/mL (Figure 8A). For REWDP-17, the emission maximum was blue-shifted from 357 to 343 nm at a concentration of 2 mg/mL (Figure 8B). The decrease in fluorescence intensity and blue shift in the emission maxima indicate the self-aggregation of the polypeptides. There was ca. 85% reduction in emission intensity at the concentration of 2 mg/mL of peptides. This large decrease is attributed to the quenching of the tryptophan fluorescence by polar functional groups (e.g., −COOH, ≡NH^+), which are brought into close proximity by the aggregation of the peptide molecules.[21] Because of the absence of tryptophan in RADA-16, we did not investigate its self-assembly in solution using fluorescence emission studies.

We reported earlier that goose eggshell matrix protein ansocalcin forms aggregates (dimer and trimer) and triggers the formation of calcite crystal aggregates.[12] It is interesting to note that the designer peptides discussed here (REWD-16 and REWDP-17) showed similar behavior in solution and in in vitro crystal growth experiments. At lower concentrations, the peptides exist in the monomeric form, whereas at higher concentration, they exist in the polymeric form. The mean diffusion coefficient, which relates to the movement

of the macromolecules in solution, is significantly lower for these peptides in the aggregated state. Thus, in the nonaggregated form, the random movement of the peptides resulted in a nonspecific interaction with the $CaCO_3$ crystals thereby inducing pits and truncation of the calcite rhombs. The generation of more nucleation sites (in the form of −COOH groups) in the peptide aggregates may be responsible for the crystal aggregates and increase in the nucleation density. The apparent lack of induction of calcite crystal aggregates by RADA-16 suggests the importance of multiplets of charged amino acids.

Thus the two designer peptides REWD-16 and REWDP-17 interact in a similar way as ansocalcin although the efficacy of the peptides is 5−10 times lower. This lower efficiency may be due to the smaller size of the peptides compared to larger intact protein molecules.

Acknowledgment. The authors thank the Singapore-MIT Alliance, National University of Singapore, Agency for Science, Technology and Research, Singapore, for financial support. We also acknowledge the technical support from the Department of Chemistry and the Department of Biological Sciences, National University of Singapore.

References and Notes

(1) (a) Arias, J. L.; Fink, D. J.; Xiao, S. Q.; Heuer, A. H.; Caplan, A. I. *Int. Rev. Cytol*. **1993**, *145*, 217−250. (b) Heuer, A. H.; Fink, D. J.; Laraia, V. J.; Arias, J. L.; Calvert, P. D.; Kendall, K.; Messing, G. L.; Blackwell, J.; Rieke, P. C.; Thompson, D. H.; Wheeler, A. P.; Veis, A.; Caplan, A. I. *Science* **1992**, *255*, 1098−1105. (c) Nys, Y.; Hincke, M. T.; Arias, J. L.; Garcia-Ruiz, J. M.; Solomon, S. E. *Poult. Avian Biol. Rev*. **1999**, *10*, 143−166. (d) Panheleux, M.; Nys, Y.; Williams, J.; Gautron, J.; Boldicke, T.; Hincke, M. T. *Poult. Sci*. **2000**, *79*, 580−588.

(2) Nys, Y.; Gautron, J.; McKee, M. D.; Garcia-Ruiz, J. M.; Hincke, M. T. *World Poult. Sci. J.* **2001**, *57*, 401−413.

(3) (a) Pines, M.; Knopov, V.; Bar, A. *Matrix Biol.* **1994**, *14*, 765−771. (b) Hincke, M. T.; Tsang, C. P. W.; Courtney, M.; Hill, V.; Narbaitz, R. *Calcif. Tissue Int.* **1995**, *56*, 578−583. (c) Hincke, M. T.; Gautron, J.; Tsang, C. P. W.; McKee, M. D.; Nys, Y. *J. Biol. Chem.* **1999**, *274*, 32915−32923.

(4) Mann, S. Crystallochemical strategies in biomineralization. In *Biomineralization: Chemical and Biochemical perspectives*; Mann, S., Webb, J., Williams R. J. P., Eds.; VHC Publisher: Weinheim, Germany, 1999; p 35.

(5) Addadi, L.; Weiner, S. *Angew. Chem., Int. Ed. Engl.* **1992**, *31*, 153−169.

(6) (a) Wheeler, A. P.; Sikes, C. S. In *Chemical Aspects of Regulation of Mineralization*; Sikes, C. S., Wheeler, A. P., Eds.; Mobile, AL, 1988; pp 9−13. (b) Wheeler, A. P.; Sikes, C. S. In *Material Synthesis Utilising Biological Process*; Rieke, P. C., Calvert, P. D., Alper, M., Eds.; Material Research Society: Pittsburgh, PA 1989; pp 45−50.

(7) Wierzbicki, A.; Sikes, C. S.; Madura, J. D.; Drake, B. *Calcif. Tissue Int.* **1994**, *54*, 133−141.

(8) Levi, Y.; Albeck, S.; Brack, A.; Weiner, S.; Addadi, L. *Chem.−Eur. J*. **1998**, *4*, 389−396.

(9) DeOliveira, D. B.; Laursen, R. A. *J. Am. Chem. Soc*. **1997**, *119*, 10627−10631.

(10) (a) Gaskin, D. J. H.; Starck, K.; Vulfson, E. N. *Biotechnol. Lett.* **2000**, *22*, 1211−1216. (b) Li, C.; Botsaris, G. D.; Kaplan, D. L. *Cryst. Growth Des*. **2002**, *2*, 387−393.

(11) (a) MacArthur, M. W.; Thornton, J. M. *J. Mol. Biol.* **1991**, *218*, 397−412. (b) Harkey, M. A.; Klueg, K.; Shepperd, P.; Raff, R. A. *Dev. Biol*. **1995**, *168*, 549−566. (c) Benson, S. C.; Wilt, F. H. In *Calcification in Biological Systems*; Bonucci, E., Ed.; CRC Press: Boca Raton, FL, 1992; pp 157−178.

(12) (a) Lakshminarayanan, R.; Valiyaveettil, S.; Kini, R. M. *Proc. Natl. Acad. Sci., U.S.A.* **2002**, *99*, 5155−5159. (b) Lakshminarayanan, R.; Valiyaveettil, S.; Rao, V. S.; Kini, R. M. *J. Biol. Chem.* **2003**, *278*, 2928−2936.

(13) Hincke, M. T. *Connect. Tissue Res.* **1995**, *31*, 227−233. (b) Mann, K.; Siedler, F. *Biochem. Mol. Biol. Int.* **1999**, *47*, 997−1007.

(14) (a) Samata, T.; Hayashi, N.; Kono, M.; Hasegawa, K.; Horita, C.; Akera, S. *FEBS Lett.* **1999**, *462*, 225−229. (b) George, A.; Bannon, L.; Sabsay, B.; Dillon, J. W.; Malone, J.; Veis, A.; Jenkins, N. A.; Gilbert, D. J.; Copeland, N. G. *J. Biol. Chem.* **1996**, *271*, 32868−32873. (c) Sarashina, I.; Endo, K. *Mar. Biotechnol.* **2001**, *3*, 362−369. (d) Testeniere, O.; Hecker, A.; Le Gurun, S.; Quennedey, B.; Graf, F.; Luquet, G. *Biochem. J.* **2002**, *361*, 327−335.

(15) (a) Moradian-Oldak, J.; Leung, W.; Fincham, A. G. *Biopolymers* **1998**, *46*, 225−238. (b) Moradian-Oldak, J.; Leung, W.; Fincham, A. G. *J. Struct. Biol*. **1998**, *122*, 320−327. (c) Killian, C. E.; Wilt, F. H. *J. Biol. Chem*. **1996**, *271*, 9150−9159. (d) Wustman, B. A.; Morse, D. E.; Evans, J. S. *Langmuir* **2002**, *18*, 9901−9906. (e) Wustman, B. A.; Santos, R.; Zhang, B.; Evans, J. S. *Biopolymers* **2002**, *65*, 362−372. (f) Zhang, B.; Wustman, B. A.; Morse, D. E.; Evans, J. S. *Biopolymers* **2002**, *63*, 358−369. (g) Zhang, B.; Xu, G. Z.; Evans, J. S. *Biopolymers* **2000**, *54*, 464−475. (h) Xu, G. Z.; Evans, J. S. *Biopolymers* **1999**, *49*, 303−312.

(16) Bergdoll, M.; Remy, M. H.; Cagnon, C.; Masson, J. M.; Dumas, P. *Structure* **1997**, *5*, 391−398.

(17) (a) Zhang, S.; Holmes, T. C.; DiPersio, C. M.; Hynes, R. O.; Su, X.; Rich, A. *Biomaterials* **1995**, *16*, 1385−1393. (b) Zhang, S. *Biotechnol. Adv.* **2002**, *20*, 321−339.

(18) Cerini, C.; Peyrot, V.; Garnier, C.; Duplan, L.; Veesler, S.; Le Caer, J. P.; Bernard, J. P.; Bouteille, H.; Michel, R.; Vazi, A.; Dupuy, P.; Michel, B.; Berland, Y.; Verdier, J. M. *J. Biol. Chem*. **1999**, *274*, 22266−22274.

(19) (a) Sreerama, N.; Woody, R. W. *Biochemistry* **1994**, *33*, 10022−10025. (b) Shankaramma, S. C.; Singh, S. K.; Sathyamurthy, A.; Balaram, P. *J. Am. Chem. Soc*. **1999**, *121*, 5360−5363.

(20) Zhang, S.; Altman, M. *React. Funct. Polym.* **1999**, *41*, 91−102.

(21) Ruddock, L. W.; Hirst, T. R.; Freedman, R. B. *Biochem. J.* **1996**, *315*, 1001−1005.

BM034101B